Energy Landscape and Phase Competition of CsV_3Sb_5, CsV_6Sb_6 and $TbMn_6Sn_6$-Type Kagome Materials

Guanghui Cai(蔡光辉)[1,2†], Yutao Jiang(姜昱韬)[1,2†], Hui Zhou(周辉)[1,2], Ze Yu(喻泽)[1,2], Kun Jiang(蒋坤)[1], Youguo Shi(石友国)[1], Sheng Meng(孟胜)[1,2,3*], and Miao Liu(刘淼)[1,3,4*]

[1]*Beijing National Laboratory for Condensed Matter Physics, and Institute of Physics, Chinese Academy of Sciences, Beijing 100190, China*
[2]*School of Physical Sciences, University of Chinese Academy of Sciences, Beijing 100190, China*
[3]*Songshan Lake Materials Laboratory, Dongguan 523808, China*
[4]*Center of Materials Science and Optoelectronics Engineering, University of Chinese Academy of Sciences, Beijing 100049, China*

(Received 24 August 2023; accepted manuscript online 8 October 2023)

Finding viable Kagome lattices is vital for materializing novel phenomena in quantum materials. In this study, we performed element substitutions on CsV_3Sb_5 with space group $P6/mmm$, $TbMn_6Sn_6$ with space group $P6/mmm$, and CsV_6Sb_6 with space group $R\bar{3}m$, as the parent compounds. Totally 4158 materials were obtained through element substitutions, and these materials were then calculated via density functional theory in high-throughput mode. Afterwards, 48 materials were identified with high thermodynamic stability ($E_{\rm hull} < 5$ meV/atom). Furthermore, we compared the thermodynamic stability of three different phases with the same elemental composition and predicted some competing phases that may arise during material synthesis. Finally, by calculating the electronic structures of these materials, we attempted to identify patterns in the electronic structure variations as the elements change. This study provides guidance for discovering promising AM_3X_5/AM_6X_6 Kagome materials from a vast phase space.

DOI: 10.1088/0256-307X/40/11/117101

The Kagome lattice[1] forms the basis for numerous unique quantum phenomena, such as spin frustration,[2] unconventional superconductivity,[3] Dirac/Weyl semimetals,[4–6] giant anomalous Hall effect,[7–9] and charge density wave order,[10–12] due to its particular spatial configuration.[13] Thus, the discovery of synthesizable real-world Kagome compounds would significantly accelerate progress in the field of quantum materials. CsV_3Sb_5, a material containing the Kagome lattice, was previously discovered,[14–16] demonstrating interesting features of flat energy bands, van Hove singularity, and Dirac point in its electronic structure. This material was also found to exhibit superconductivity below 2.5 K,[17] making it a potential quantum material candidate, with proposed applications, such as energy-efficient nano-electronic devices, as suggested by Zheng *et al.*[18] In addition to CsV_3Sb_5, RbV_3Sb_5 and KV_3Sb_5[19,20] were identified as potential systems for exploring novel quantum phenomena, given their similar atomic and electronic structures.

Aside from compounds similar to CsV_3Sb_5, researchers have revealed the synthesizable Kagome lattice-based compound CsV_6Sb_6,[21] which has a more complex bilayer structure. This finding presents new possibilities for studying a range of topological non-trivialities in bilayer Kagome materials. Interestingly, while CsV_6Sb_6 shares the stoichiometry of another Kagome material, $TbMn_6Sn_6$,[22–24] their crystal structures differ. CsV_6Sb_6 belongs to the $R\bar{3}m$ space group, while $TbMn_6Sn_6$ falls into the $P6/mmm$ space group. Detailed comparisons of the crystal structures of CsV_3Sb_5, CsV_6Sb_6, and $TbMn_6Sn_6$ are depicted in Figs. 1(a)–1(c).

Theoretical prediction by computer can greatly accelerate the discovery process of materials. For example, it expedited the *in silico* design of the Mg-ion battery[25,26] and N-containing ternary compound,[27] and the theoretical predictions are all confirmed by experiments. In this Letter, we implement the same technique for CsV_3Sb_5, CsV_6Sb_6, and $TbMn_6Sn_6$-based systems (denoted as CVS135-type, CVS166-type, and TMS166-type systems, respectively, for convenience throughout this study), with the aim of methodically identifying potential Kagome materials from these systems. In the present study, we expand a previous work,[28] which only analyzed CVS135-type compounds, by investigating a broader structural phase space (three structure templates), and provide a thorough analysis of trends and insight into understanding phase competition in these compounds.

To elaborate, we initially subjected the elements in CsV_3Sb_5, CsV_6Sb_6, and $TbMn_6Sn_6$ crystal structures to substitution, resulting in 4158 possible materials. We then employed high-throughput computation to calculate the formation energy, giving us the thermodynamic stability of all these compounds. Following a comprehensive search, we identified 48 compounds with robust thermodynamic stability ($E_{\rm hull} < 5$ meV/atom), which are listed in Ta-

†These authors contributed equally to this work.
*Corresponding authors. Email: smeng@iphy.ac.cn; mliu@iphy.ac.cn

ble 1. Our findings show that CVS135-type, CVS166-type, and TMS166-type structures have distinct preferences for certain chemical elements. For instance, several stable TMS166-type compounds emerged when the Tb site was replaced by H/Li/Na, while introducing elements such as K/Cs/Ru could bring about the stability of the compound in CVS135-type and CVS166-type structures. We also find that the CVS135-type compound is more prevalent since the CVS166-type compound typically exhibits less stability. Exceptions to this include compounds such as $RbFe_6Sb_6$, $RbTc_6Sb_6$, $CsFe_6Sb_6$, $CsTc_6Sb_6$, and $CsTc_6Ge_6$. The presence of phase competition in K–Ti–Bi, Rb–Ti–Bi, Cs–Ti–Bi, and Cs–Pd–Pb compounds indicates that the synthesis may be more nuanced, even if these materials are theoretically stable. This work demonstrates a standard method for identifying new synthesizable compounds swiftly and affordably, thereby shedding light on revolutionary techniques within the domain of physical science.

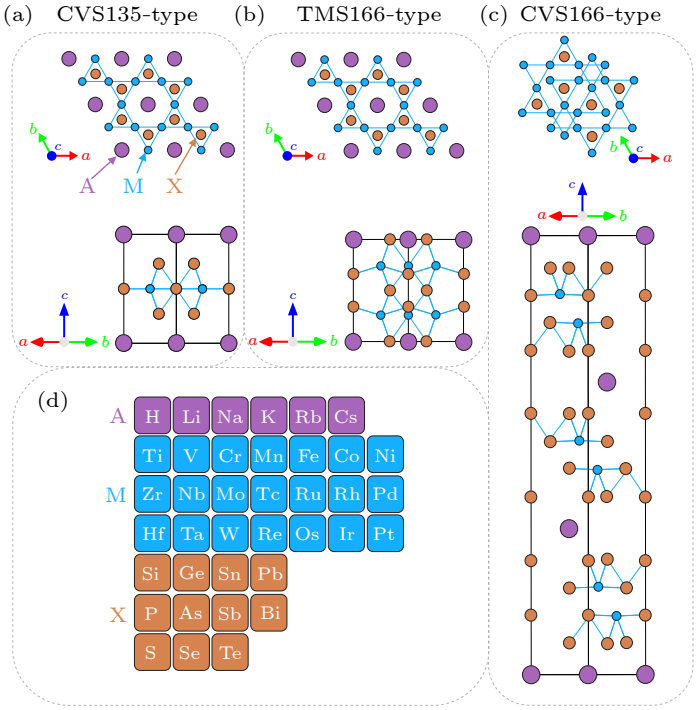

Fig. 1. Three types of Kagome materials with distinct structural templates: (a) CsV_3Sb_5-type, space group $P6/mmm$, denoted as CVS135-type structure, (b) $TbMn_6Sn_6$-type, space group $P6/mmm$, denoted as TMS166-type structure, (c) CsV_6Sb_6-type, space group $R\bar{3}m$, denoted as CVS166-type structure. When substituting the elements in the above three structural templates, the selected elements are displayed in (d).

Methodology. In this study, we employed a high-throughput workflow to calculate a total of 4158 Kagome compounds with different compositions and space groups. Specifically, we calculated 1386 CVS135-type compounds (whose composition can be represented as AM_3X_5) with space group $P6/mmm$, 1386 TMS166-type compounds (AM_6X_6) with space group $P6/mmm$, and 1386 CVS166-type compounds (AM_6X_6) with space group $R\bar{3}m$. Among them, the "A" element comes from the element set composed of purple squares in Fig. 1(d), the "M" element comes from the element set composed of indigo squares, and the "X" element comes from the element set composed of orange squares. All calculations were carried out under the same parameters as given below.

The Vienna *ab initio* Simulation Package (VASP)[29,30] code with the projector augmented wave method[31,32] was used to realize the density functional theory calculations.[33] We choose the generalized gradient approximation of Perdew–Burke–Ernzerhof[34] to describe the exchange and correlation energy density function. We did not consider the Hubbard U corrections as all those systems are metallic compounds. The conjugate gradient scheme was used to optimize the atomic structures. The cutoff energy was chosen to be 520 eV. The gamma-centered k-mesh was used to sample the Brillouin zone during the calculation at the density of 100 k-points/Å^{-3}. All the calculations were initiated with ferromagnetism throughout this study to yield their ground-state spin polarization within the primitive cell configuration, but we did not include the relativistic spin-orbital coupling effect in this study. The energy convergence criterion of the self-consistency was set at 5×10^{-6} eV.

Results and Discussion. The synthesizability of a compound primarily depends on its thermodynamic stability and the kinetics during its growth process. This means that a compound thermodynamically competes with all potential phases in the same chemical space and eventually settles into the energetically favorable phases. Consequently, determining the existence probability of a compound would become easier if the formation en-

ergies of all stable compounds are known. From computational databases, such as the Materials Project,[35] AFLOW[36] and Atomly,[37] the energy landscape of numerous chemical spaces is readily available, making it easier for us to assess the thermodynamic stability of a given compound.[38–40]

In particular, the formation energy of a compound, also known as the standard enthalpy of formation, is defined as the enthalpy change when a substance forms from its pure elements under identical conditions.[41] A negative formation energy signifies energy released by the reaction and relative stability of the compound, and vice versa. The most stable compounds in a chemical system delineate the lower boundary of formation energies or the energy convex hull in the chemical system, given that the formation energies of stable compounds are negative. The distance between a compound's formation energy and the energy convex hull, also referred to as "the energy above the hull ($E_{\rm hull}$)", serves as a valuable metric for verifying the thermodynamic stability of the compound. Essentially, $E_{\rm hull}$ denotes the driven force in energy to decompose a compound.[42–44]

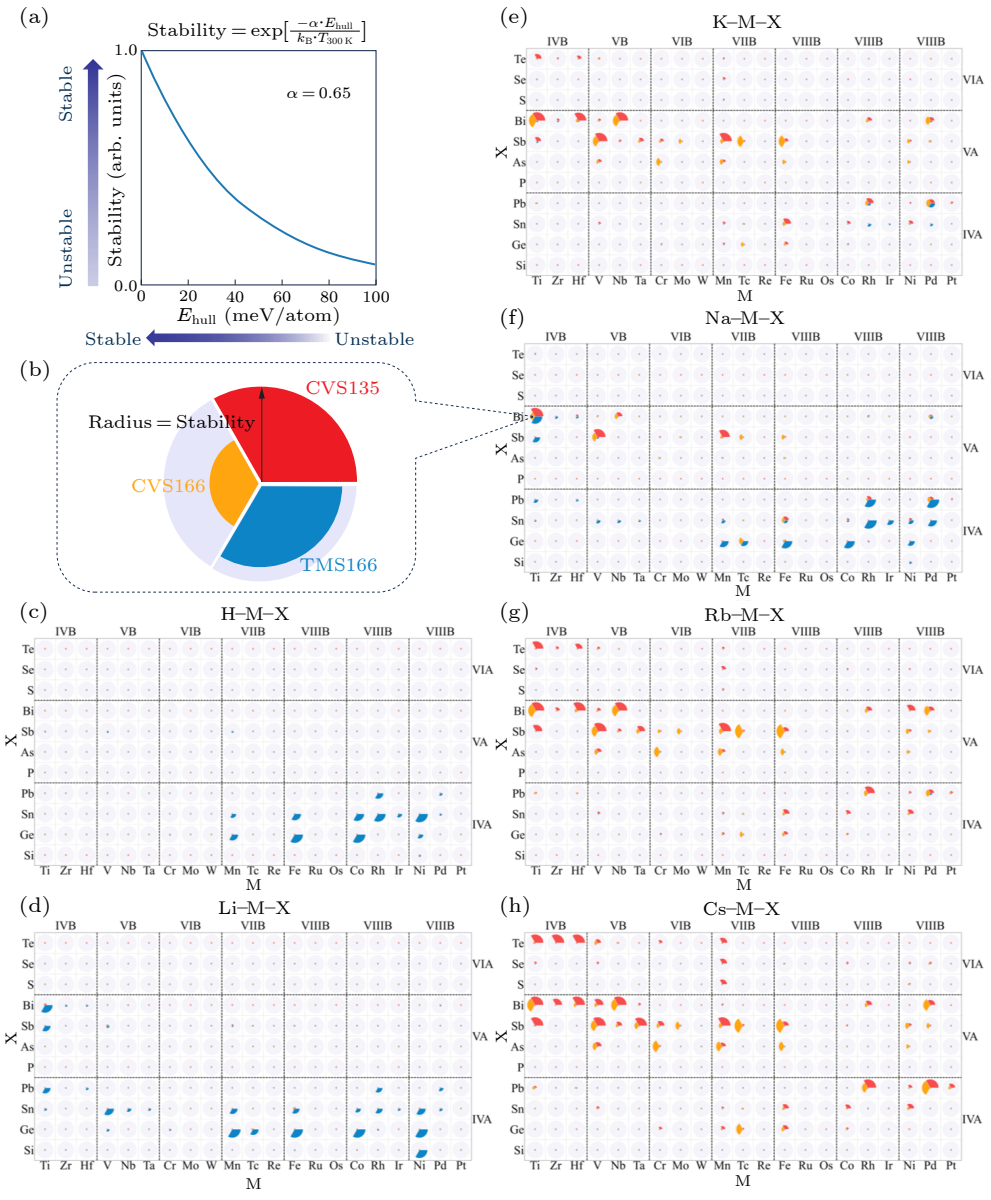

Fig. 2. Thermodynamic stability of three types of Kagome structures in expanded chemical space. We first define the stability measure of a compound based on the $E_{\rm hull}$ and Boltzmann distribution, as shown in (a). Stability = 1.0 stands for stable compounds, Stability = 0.61 corresponds to $E_{\rm hull}$ = 20 meV/atom and Stability = 0.08 corresponds to $E_{\rm hull}$ = 100 meV/atom. (b) Three sectors of the pie chart represent three Kagome crystalline types: the red sector represents CVS135-type compound with space group $P6/mmm$, the blue sector represents TMS166-type compound with space group $P6/mmm$, and the yellow sector represents CVS166-type compound with space group $R\bar{3}m$. Radius of each sector denotes the thermodynamic stability of each compound as defined in (a). The larger the radius of a sector is, the more stable the compound is. (c)–(h) The thermodynamic stability of the H–M–X, Li–M–X, Na–M–X, K–M–X, Rb–M–X, and Cs–M–X, respectively.

In this study, we first expand the chemical space of the AM_6X_6, covering both the $R\bar{3}m$ and $P6/mmm$ structures, totaling 2772 compounds. Then, the $E_{\rm hull}$ is derived for all the compounds by plugin data from the Atomly database. The AM_3X_5 (1386 structures) compounds were previously investigated by Jiang *et al.* and these data are included for comparison.[28] All the data can be accessed from atomly.net.[37]

In Fig. 2, we plot the $E_{\rm hull}$ of the three different structures mentioned in the article with the same element composition in each circle and use this to elucidate their stability and phase competition. The CVS135-type (space group $P6/mmm$) compounds are plotted in red, whereas the CVS166-type (space group $R\bar{3}m$) compounds are shown in yellow, and the TMS166-type (space group $P6/mmm$) compounds are plotted in blue. The radius of each sector in the figure represents the magnitude of stability; the larger the radius, the higher the stability. It is found from Fig. 2 that among the hydrogen-containing, lithium-containing, and sodium-containing compounds, TMS166-type compounds with space group $P6/mmm$ have more thermodynamically stable structures than the other two types of Kagome structures. In the compounds containing potassium, rubidium, and cesium, there are hardly any TMS166-type compounds but many CVS135-type compounds with space group $P6/mmm$ and CVS166-type compounds with space group $R\bar{3}m$. Therefore, the stability of those compounds is closely element dependent.

From Fig. 2, it can be seen that the theoretical calculation is indeed in good agreement with the experiments. For example, CsV_3Sb_5,[16] RbV_3Sb_5[45] and KV_3Sb_5[20] (CVS135-type compounds with space group $P6/mmm$), $LiMn_6Sn_6$[8] (TMS166-type compounds with space group $P6/mmm$), and KV_6Sb_6, RbV_6Sb_6 and CsV_6Sb_6[46] (CVS166-type compounds with space group $R\bar{3}m$) are thermodynamically stable and thus synthesizable. Therefore, the method and treatment employed in this study is reliable. As shown in Fig. 2, there are several new compounds with good thermodynamic stability ($E_{\rm hull} < 5$ meV/atom). They are KTi_6Bi_6, $RbTi_6Bi_6$, $RbFe_6Sb_6$, $RbTc_6Sb_6$, $CsTi_6Bi_6$, $CsFe_6Sb_6$, $CsTc_6Sb_6$, $CsTc_6Ge_6$, and $CsPd_6Pb_6$ in CVS166-type structure and HFe_6Ge_6, HCo_6Ge_6, HNi_6Sn_6, HRh_6Sn_6, $LiTi_6Bi_6$, $LiFe_6Ge_6$, $LiNi_6Ge_6$, $LiNi_6Si_6$, $NaRh_6Pb_6$, $NaRh_6Sn_6$, and $NaPd_6Pb_6$ in TMS166-type structure, which require future experimental confirmation. Table 1 lists the details of these low $E_{\rm hull}$ Kagome materials, including their chemical formula, the structure type they belong to, the ID number in the Atomly database,[37] the $E_{\rm hull}$ value of materials, and whether the material has been experimentally synthesized. Among them, the materials that have not been synthesized by experiments are very promising materials that can be synthesized in the future.

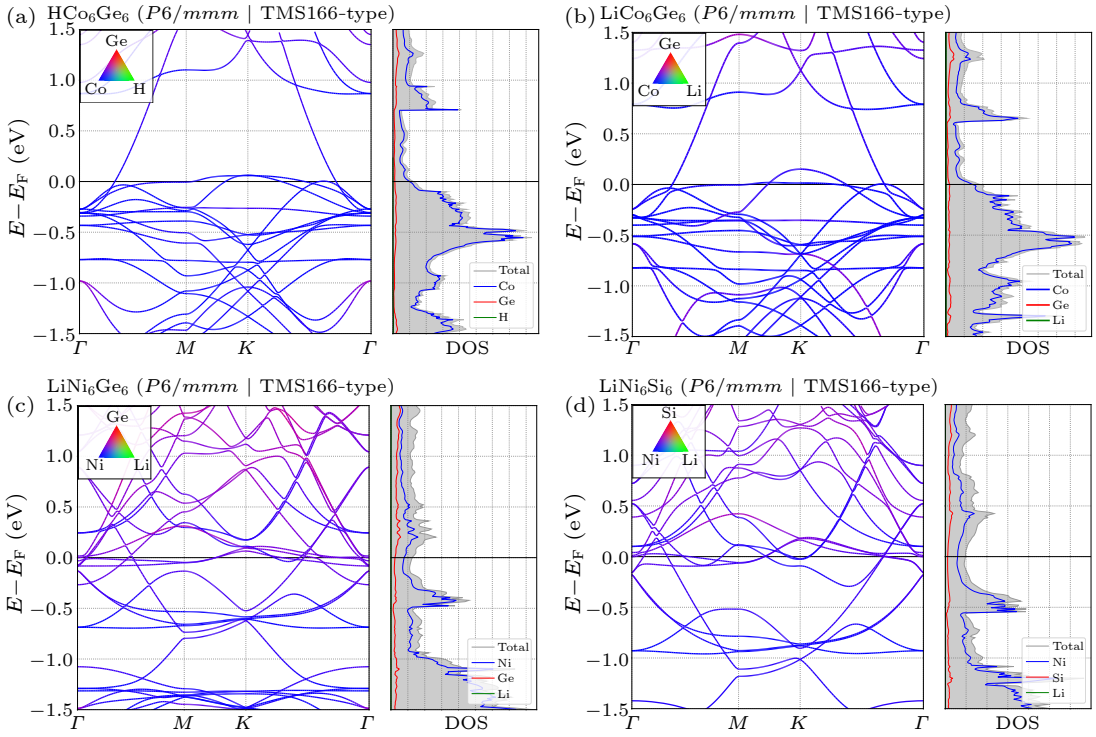

Fig. 3. Electronic structures of representative compounds of TMS166-type structures with $E_{\rm hull} < 5$ meV/atom: (a) band structure of HCo_6Ge_6, (b) band structure of $LiCo_6Ge_6$, (c) band structure of $LiNi_6Ge_6$, (d) band structure of $LiNi_6Si_6$.

The phase competition can also be seen in Fig. 2. Here, we only list two out-of-phase $E_{\rm hull}$ which are both below 5 meV/atom. The cases in which the $E_{\rm hull}$ of two different phases are both lower than 10 meV/atom can be found in Table S1 in the Supporting Information. For example, both K–Ti–Bi in CVS166-type structure and CVS135-type structure exhibit relative stability. This is evident from their formation energy, with the CVS166-type structure

having an E_{hull} of 3.79 meV/atom and the CVS135-type structure being in its thermodynamic ground state with an E_{hull} of 0.0 meV/atom. The difference in formation energy between these two structures is only 3.79 meV/atom. Hence, this presents an additional challenge for synthesizing the desired phase. Similarly, this phase competition can also be found in compounds containing Rb–Ti–Bi, Cs–Ti–Bi and Cs–Pd–Pb elements, and they are all a competition between CVS135-type and CVS166-type structures.

Table 1. List of top 48 stable compounds ($E_{\text{hull}} < 5$ meV/atom). The chemical formula, structure type, ID of the compound in atomly.net,[37] E_{hull} of the compound and references of the experiments (if available) of these compounds are listed.

Chemical formula	Structure type	Atomly ID	E_{hull}(meV/atom)	Experimental References
HFe_6Ge_6	TMS166	1000301638	0.00	
HCo_6Ge_6	TMS166	1000301649	0.00	
HNi_6Sn_6	TMS166	1000301661	0.68	
HRh_6Sn_6	TMS166	1000301727	3.35	
$LiTi_6Bi_6$	TMS166	1000301823	4.84	
$LiMn_6Ge_6$	TMS166	3001812095	0.00	
$LiFe_6Ge_6$	TMS166	3001812096	0.00	[47]
$LiCo_6Ge_6$	TMS166	0000060277	0.00	[48]
$LiNi_6Ge_6$	TMS166	0000043146	0.00	[48]
$LiNi_6Si_6$	TMS166	0000102969	2.72	[48]
$NaTi_3Bi_5$	CVS135	1000299281	0.00	
NaV_3Sb_5	CVS135	1000299291	2.02	
$NaRh_6Pb_6$	TMS166	1000302186	4.79	
$NaRh_6Sn_6$	TMS166	1000302185	0.00	
$NaPd_6Pb_6$	TMS166	1000302197	0.00	
KTi_3Bi_5	CVS135	1000299512	0.00	
KTi_6Bi_6	CVS166	1000300902	3.79	
KV_3Sb_5	CVS135	1000299522	0.00	[15]
KMn_3Sb_5	CVS135	1000299544	0.00	
KNb_3Bi_5	CVS135	1000299600	0.00	
KHf_3Bi_5	CVS135	1000299666	2.99	
$RbTi_3Bi_5$	CVS135	1000299743	0.00	[49]
$RbTi_6Bi_6$	CVS166	1000301133	4.08	
RbV_3Sb_5	CVS135	1000299753	0.00	[15]
$RbMn_3Sb_5$	CVS135	1000299775	0.00	
$RbFe_6Sb_6$	CVS166	1000301264	0.00	
$RbNb_3Bi_5$	CVS135	1000299831	0.00	
$RbTc_6Sb_6$	CVS166	1000301242	0.00	
$RbHf_3Bi_5$	CVS135	1000299897	0.00	
$CsTi_3Bi_5$	CVS135	1000299974	0.00	[49]
$CsTi_6Bi_6$	CVS166	1000301364	4.48	
$CsTi_3Te_5$	CVS135	1000299981	0.00	
$CsTi_3Sb_5$	CVS135	1000299973	0.00	
CsV_3Sb_5	CVS135	1000299984	0.00	[15]
$CsMn_3Sb_5$	CVS135	1000300006	0.00	
$CsFe_6Sb_6$	CVS166	1000301495	0.00	
$CsFe_3Sn_5$	CVS135	1000300021	0.00	
$CsFe_3Ge_5$	CVS135	1000300020	0.20	
$CsZr_3Te_5$	CVS135	1000300058	0.00	
$CsNb_3Bi_5$	CVS135	1000300062	0.00	
$CsTc_6Sb_6$	CVS166	1000301473	0.00	
$CsTc_6Ge_6$	CVS166	1000301468	0.00	
$CsRh_3Pb_5$	CVS135	1000300110	0.00	
$CsPd_3Pb_5$	CVS135	1000300121	0.00	
$CsPd_6Pb_6$	CVS166	1000301569	1.00	
$CsHf_3Bi_5$	CVS135	1000299897	0.00	
$CsHf_3Te_5$	CVS135	1000300135	0.00	
$CsTa_3Sb_5$	CVS135	1000300138	2.27	

Previously, we used a similar method to explore the thermodynamic stability of the CVS135-type Kagome materials,[28] and a couple of predicted phases, e.g., $CsTi_3Bi_5$ and $RbTi_3Bi_5$ have been successfully synthesized.[49,50] In this study, as we further expanded the chemical space of these systems, we found that the newly added compound may have even lower formation energy to break the existing convex hull, resulting in the

E_{hull} rapidly increasing to larger values. Therefore, the stable compounds found in previous works may become less stable as another new stable phase is added. For example, CsV_3Bi_5 was previously found to be a stable structure, but the newly added compound in Cs–V–Bi chemical phase space is found to have even smaller formation energy and is indeed the new stable compound.

We then calculated the full electronic structures, including DOS and band structure, for all 4158 structures generated by replacing elements in the three structural templates mentioned above. All the data can be accessed from atomly.net.[37] This analysis not only helps in discovering novel topological materials but also guides band engineering using different metal elements as dopants.[51]

To investigate the effects of different elements on different sites in AM_6X_6 Kagome compounds with TMS166-type structures, we selected four structures with good thermodynamic stability ($E_{\text{hull}} < 5$ meV/atom) using a controlled variable method, namely HCo_6Ge_6 (Atomly ID: 1000301649), $LiCo_6Ge_6$ (Atomly ID: 0000060277), $LiNi_6Ge_6$ (Atomly ID: 0000043146) and $LiNi_6Si_6$ (Atomly ID: 0000102969). By comparing the electronic structures of HCo_6Ge_6 [Fig. 3(a)] and $LiCo_6Ge_6$ [Fig. 3(b)], we found that the A-site element has little influence on the compound's electronic structure near the Fermi level. This is because the A-site element's energy level is located deeply within the Fermi surface and cannot have a significant impact on the bands near the Fermi level. Through a comparison of the electronic structures of $LiCo_6Ge_6$ [Fig. 3(b)] and $LiNi_6Ge_6$ [Fig. 3(c)], it was observed that $LiNi_6Ge_6$ exhibits characteristics of electron doping in comparison to $LiCo_6Ge_6$, causing its Dirac cone and van Hove singularity to shift closer to the Fermi surface, resulting in a corresponding downward shift in the position of the flat band. We also observed a difference in the electronic structures of $LiNi_6Ge_6$ [Fig. 3(c)] and $LiNi_6Si_6$ [Fig. 3(d)]. The position of the Dirac cone at the K point in $LiNi_6Si_6$ is higher than in $LiNi_6Ge_6$. This difference can be attributed to the higher electronegativity of Si compared to Ge. The greater electronegativity of silicon causes it to attract more electrons, leading to a hole-doping effect in $LiNi_6Si_6$ and an overall upward shift of the band.

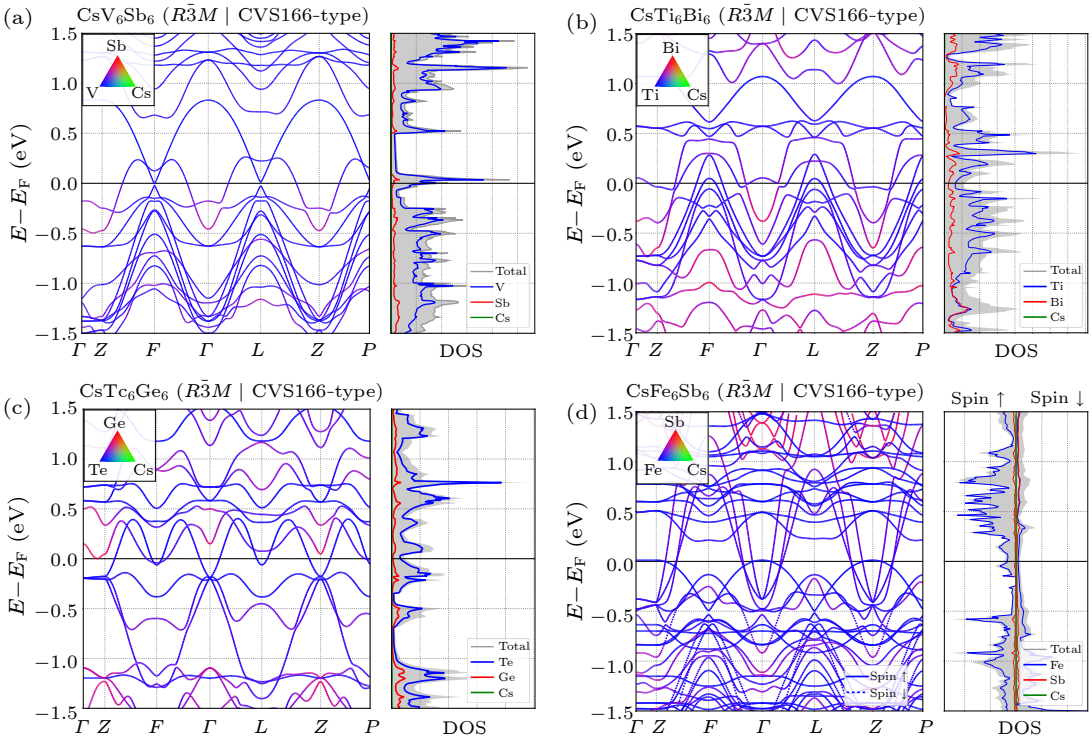

Fig. 4. Electronic structures of representative compounds of CVS166-type structures with $E_{\text{hull}} < 5$ meV/atom (Exception is the E_{hull} of CaV_6Sb_6, which is 11.96 meV/atom, and it is shown in Table S1 in the Supporting Information). (a) Band structure of CsV_6Sb_6, (b) band structure of $CsTi_6Bi_6$, (c) band structure of $CsTc_6Ge_6$, (d) band structure of $CsFe_6Sb_6$.

The CsV_6Sb_6 (Atomly ID: 1000301396) compound with space group $R\bar{3}m$ exhibits a significant feature of multiple linear band crossings forming type-Ⅱ Dirac nodal lines near the Fermi level in the band structure.[46] Regarding the band structures, we found that the bilayer CVS166-type compounds[52] exhibit a much simpler band topology compared to their previously studied single-layer CVS135-type counterparts.[53] Fewer bands cross the Fermi level, indicating simpler Fermi surface structures, and no ordinary van Hove singularity[54] or type-I Dirac point like those found near the Fermi level in CVS135-type compounds. These differences may be attributed to the interlayer interactions of Kagome bilayers present in CVS166-type compounds but absent in CVS135-type compounds.

To further demonstrate the changing characteristics of the energy bands of the CVS166-type compounds (AM_6X_6 with space group $R\bar{3}m$), we present in Fig. 4 the electronic structures of representative compounds. We also

observed that the A-site element has little influence on the compound's electronic structure near the Fermi level. This observation is supported by the band structure and DOS plots of all these compounds in Fig. 4, which indicate that the states near the Fermi level are mostly dominated by the d orbital electrons of the M-site element, with almost no electronic state from the A-site element found near the Fermi level. Therefore, only Cs-containing compounds are shown in Fig. 4. First, the band structure of CsV_6Sb_6 [Fig. 4(a)] exhibits multiple type-Ⅱ Dirac points just above the Fermi level near the F and L points, which is consistent with previous studies and verifies the accuracy of our results. Second, the band structures of $CsTi_6Bi_6$ (Atomly ID: 1000301364) and $CsTc_6Ge_6$ (Atomly ID: 1000301468) in Figs. 4(b) and 4(c), respectively, can be regarded as the band structures of hole-doped and electron-doped CsV_6Sb_6. We note that $CsTi_6Bi_6$ exhibits more hole-like bands near the Fermi level around the F and L points. However, these bands rise in energy along with the electron-like bands, resulting in less energy dispersion and the disappearance of linear band crossings near the Fermi level. For $CsTc_6Ge_6$, more electron-like bands are present near the Fermi level around the F and L points, and the linear band crossings around the F and L points occur more below the Fermi level due to the higher number of valence electrons compared to CsV_6Sb_6, which raises the Fermi level. The band structure of $CsFe_6Sb_6$ (Atomly ID: 1000301495) in Fig. 4(d) shows ferromagnetism, and it exhibits linear band crossings around the F and L points at approximately 0.4 eV below the Fermi level for bands of spin-down electrons exhibiting the characteristics of a Weyl point,[55] but no such crossing is found in the bands of spin-up electrons, which can be used as a model system to study the interplay between topological superconductivity and magnetism.[56,57]

In addition to the band structure discussion, it is noteworthy that the compounds in Fig. 4(d) with linear band crossings around the F and L points, namely CsV_6Sb_6 and $CsFe_6Sb_6$, exhibit a nearly zero DOS at the energy where these crossings occur, a characteristic of a Weyl semimetal. Furthermore, all the band topological features of the Cs-containing compounds discussed above are also observed in their K-containing and Rb-containing counterparts. Taken together, given that AFe_6Sb_6 (A = K, Rb, Cs) possesses similar band characteristics to $CsFe_6Sb_6$, it is highly probable that these compounds are topological semimetals with type-Ⅱ nodal line fermions, like $CsFe_6Sb_6$, with space group $R\bar{3}m$. However, to achieve precise topological classification of these compounds, additional comprehensive investigations are necessary, such as performing band symmetry group analysis, conducting band structure calculations with SOC, simulating edge states, etc. Consequently, it is highly anticipated that further research on the CVS166-type compounds suggested in this study will provide a more comprehensive and robust understanding of their band topology.

In summary, we have found 13 structures, which are HFe_6Ge_6, HCo_6Ge_6, HNi_6Sn_6, HRh_6Sn_6, $LiTi_6Bi_6$, $LiMn_6Ge_6$, $LiFe_6Ge_6$, $LiCo_6Ge_6$, $LiNi_6Ge_6$, $LiNi_6Si_6$, $NaRh_6Pb_6$, $NaRh_6Sn_6$, and $NaPd_6Pb_6$, with good thermodynamic stability ($E_{\rm hull}$ less than 5 meV/atom) from 1386 structures generated from the parent structure of $TbMn_6Sn_6$ with space group $P6/mmm$. Out of the 1386 structures generated from the parent structure of CsV_6Sb_6 with space group $R\bar{3}m$, there are nine structures exhibiting excellent thermodynamic stability with an $E_{\rm hull}$ of less than 5 meV/atom. They are KTi_6Bi_6, $RbTi_6Bi_6$, $RbFe_6Sb_6$, $RbTc_6Sb_6$, $CsTi_6Bi_6$, $CsFe_6Sb_6$, $CsTc_6Sb_6$, $CsTc_6Ge_6$, and $CsPd_6Pb_6$. Since some of the synthesized Kagome materials have higher $E_{\rm hull}$ such as $LiMn_6Sn_6$ (Atomly ID: 1000301858) and CsV_6Sb_6 (Atomly ID: 1000301396), both have $E_{\rm hull}$ greater than 5 meV/atom, and it is highly likely that more stable compounds can be materialized for slightly larger $E_{\rm hull}$. They are all listed in Table S1 in the Supporting Information. We also point out that some materials, despite their thermodynamic stability, may pose challenges with regard to syntheses due to the competition between different phases since these phases have almost the same $E_{\rm hull}$. It is hopeful that this work will expand the scope of research on Kagome materials and lead to the discovery of more novel topological and superconducting materials.

Acknowledgments. This work was supported by the Chinese Academy of Sciences (Grant Nos. CAS-WX2023SF-0101, ZDBS-LY-SLH007 and XDB33020000) and the National Key R&D Program of China (Grant No. 2021YFA0718700). The computational resource was provided by the Platform for Data-Driven Computational Materials Discovery of the Songshan Lake laboratory.

References

[1] Syozi I 1951 *Prog. Theor. Phys.* **6** 306
[2] Nocera D G, Bartlett B M, Grohol D, Papoutsakis D, and Shores M P 2004 *Chem.: A Eur. J.* **10** 3850
[3] Guguchia Z, Mielke C, Das D, Gupta R, Yin J X, Liu H, Yin Q, Christensen M H, Tu Z, Gong C, Shumiya N, Hossain M S, Gamsakhurdashvili T, Elender M, Dai P, Amato A, Shi Y, Lei H C, Fernandes R M, Hasan M Z, Luetkens H, and Khasanov R 2023 *Nat. Commun.* **14** 153
[4] Wu Z and Wang Y 2022 *Phys. Rev. B* **106** 214510
[5] Zhang X, Jin L, Dai X, and Liu G 2017 *J. Phys. Chem. Lett.* **8** 4814
[6] Zhang Q, Zhang Y, Matsuda M, Garlea V O, Yan J, McGuire M A, Tennant D A and Okamoto S 2022 *J. Am. Chem. Soc.* **144** 14339
[7] Zhou H, Liu H, Ji H, Li X, Meng S, and Sun J T 2023 *npj Quantum Mater* **8** 16
[8] Chen D, Le C, Fu C, Lin H, Schnelle W, Sun Y, and Felser C 2021 *Phys. Rev. B* **103** 144410
[9] Liu E, Sun Y, Kumar N, Muechler L, Sun A, Jiao L, Yang S Y, Liu D, Liang A, Xu Q, Kroder J, Süß V, Borrmann H, Shekhar C, Wang Z, Xi C, Wang W, Schnelle W, Wirth S, Chen Y, Goennenwein S T B, and Felser C 2018 *Nat. Phys.* **14** 1125
[10] Zhao Y, Nie Z, Hong H, Qiu X, Han S, Yu Y, Liu M, Qiu X, Liu K, Meng S, Tong L, and Zhang J 2023 *Nat. Commun.* **14** 2223
[11] Teng X, Chen L, Ye F, Rosenberg E, Liu Z, Yin J X, Jiang Y X, Oh J S, Hasan M Z, Neubauer K J, Gao B, Xie Y, Hashimoto M, Lu D, Jozwiak C, Bostwick A, Rotenberg E, Birgeneau R J, Chu J H, Yi M, and Dai P 2022 *Nature* **609** 490
[12] Tan H, Liu Y, Wang Z, and Yan B 2021 *Phys. Rev. Lett.* **127** 46401
[13] Li M, Wang Q, Wang G, Yuan Z, Song W, Lou R, Liu Z, Huang Y, Liu Z, Lei H, Yin Z, and Wang S 2021 *Nat. Commun.* **12** 3129

[14] Ni S, Ma S, Zhang Y, Yuan J, Yang H, Lu Z, Wang N, Sun J, Zhao Z, Li D, Liu S, Zhang H, Chen H, Jin K, Cheng J, Yu L, Zhou F, Dong X, Hu J, Gao H J, and Zhao Z 2021 *Chin. Phys. Lett.* **38** 057403

[15] Ortiz B R, Gomes L C, Morey J R, Winiarski M, Bordelon M, Mangum J S, Oswald I W H, Rodriguez-Rivera J A, Neilson J R, Wilson S D, Ertekin E, McQueen T M, and Toberer E S 2019 *Phys. Rev. Mater.* **3** 094407

[16] Ortiz B R, Teicher S M L, Hu Y, Zuo J L, Sarte P M, Schueller E C, Abeykoon A M M, Krogstad M J, Rosenkranz S, Osborn R, Seshadri R, Balents L, He J, and Wilson S D 2020 *Phys. Rev. Lett.* **125** 247002

[17] Zhao H, Li H, Ortiz B R, Teicher S M L, Park T, Ye M, Wang Z, Balents L, Wilson S D, and Zeljkovic I 2021 *Nature* **599** 216

[18] Zheng G, Tan C, Chen Z, Wang M, Zhu X, Albarakati S, Algarni M, Partridge J, Farrar L, Zhou J, Ning W, Tian M, Fuhrer M S, and Wang L 2023 *Nat. Commun.* **14** 678

[19] Jiang K, Wu T, Yin J X, Wang Z, Hasan M Z, Wilson S D, Chen X, and Hu J 2023 *Natl. Sci. Rev.* **10** nwac199

[20] Jiang Y X, Yin J X, Denner M M, Shumiya N, Ortiz B R, Xu G, Guguchia Z, He J, Hossain M S, Liu X, Ruff J, Kautzsch L, Zhang S S, Chang G, Belopolski I, Zhang Q, Cochran T A, Multer D, Litskevich M, Cheng Z J, Yang X P, Wang Z, Thomale R, Neupert T, Wilson S D, and Hasan M Z 2021 *Nat. Mater.* **20** 1353

[21] Yang Y, Fan W, Zhang Q, Chen Z, Chen X, Ying T, Wu X, Yang X, Meng F, Li G, Li S, Gu L, Qian T, Schnyder A P, Guo J G, and Chen X 2021 *Chin. Phys. Lett.* **38** 127102

[22] Li R S, Zhang T, Ma W, Xu S X, Wu Q, Yue L, Zhang S J, Liu Q M, Wang Z X, Hu T C, Zhou X Y, Wu D, Dong T, Jia S, Weng H, and Wang N L 2023 *Phys. Rev. B* **107** 045115

[23] Jones D C, Das S, Bhandari H, Liu X, Siegfried P, Ghimire M P, Tsirkin S S, Mazin I I, and Ghimire N J 2022 arXiv:2203.17246 [cond-mat.str-el]

[24] Wenzel M, Tsirlin A A, Iakutkina O, Yin Q, Lei H C, Dressel M, and Uykur E 2022 *Phys. Rev. B* **106** L241108

[25] Liu M, Rong Z, Malik R, Canepa P, Jain A, Ceder G, and Persson K A 2015 *Energy Environ. Sci.* **8** 964

[26] Liu M, Jain A, Rong Z, Qu X, Canepa P, Malik R, Ceder G, and Persson K A 2016 *Energy Environ. Sci.* **9** 3201

[27] Sun W, Bartel C J, Arca E, Bauers S R, Matthews B, Orvañanos B, Chen B R, Toney M F, Schelhas L T, Tumas W, Tate J, Zakutayev A, Lany S, Holder A M, and Ceder G 2019 *Nat. Mater.* **18** 732

[28] Jiang Y, Yu Z, Wang Y, Lu T, Meng S, Jiang K, and Liu M 2022 *Chin. Phys. Lett.* **39** 047402

[29] Kresse G and Furthmiiller J 1996 *Comput. Mater. Sci.* **6** 15

[30] Kresse G and Furthmu J 1996 *Phys. Rev. B* **54** 11169

[31] Blöchl P E *Phys. Rev. B* **50** 17953

[32] Kresse G and Joubert D 1999 *Phys. Rev. B* **59** 1758

[33] Kohn W and Sham L J 1965 *Phys. Rev.* **140** A1133

[34] Perdew J P, Burke K, and Ernzerhof M 1996 *Phys. Rev. Lett.* **77** 3865

[35] Jain A, Ong S P, Hautier G, Chen W, Richards W D, Dacek S, Jain A, Ong P, Hautier G, Chen W, Gunter D, Skinner D, Ceder G, and Persson K A 2013 *APL Mater.* **1** 011002

[36] Esters M, Oses C, Divilov S, Eckert H, Friedrich R, Hicks D, Mehl M J, Rose F, Smolyanyuk A, Calzolari A, Campilongo X, Toher C, and Curtarolo S 2023 *Comput. Mater. Sci.* **216** 111808

[37] Liu M and Meng S 2023 *Sci. Sin. Chim.* **53** 19

[38] Xie F, Lu T, Yu Z, Wang Y, Wang Z, Meng S, and Liu M 2023 *Chin. Phys. Lett.* **40** 057401

[39] Liang Y, Chen M, Wang Y, Jia H, Lu T, Xie F, Cai G, Wang Z, Meng S, and Liu M 2023 *Sci. China Mater.* **66** 343

[40] Lu T, Wang Y, Cai G, Jia H, Liu X, Zhang C, Meng S, and Liu M 2023 *Mater. Futures* **2** 015001

[41] Jain A, Hautier G, Ong S P, Moore C J, Fischer C C, Persson K A, and Ceder G 2011 *Phys. Rev. B* **84** 045115

[42] Ong S P, Jain A, Hautier G, Kang B, and Ceder G 2010 *Electrochem. Commun.* **12** 427

[43] Sun W, Dacek S T, Ong S P, Hautier G, Jain A, Richards W D, Gamst A C, Persson K A, and Ceder G 2016 *Sci. Adv.* **2** e1600225

[44] Barber C B, Dobkin D P, and Huhdanpaa H 1996 *ACM Trans. Math. Softw.* **22** 469

[45] Yin Q, Tu Z, Gong C, Fu Y, Yan S, and Lei H 2021 *Chin. Phys. Lett.* **38** 037403

[46] Yang Y, Wang R, Shi M Z, Wang Z, Xiang Z, and Chen X H 2021 *Phys. Rev. B* **104** 245128

[47] E Welk H-U S 2006 *Z. Anorg. Allg. Chem.* **632** 1917

[48] Buchholz W and Schuster H U 1978 *Z. Naturforsch. B* **33** 877

[49] Yang H, Zhao Z, Yi X W, Liu J, You J Y, Zhang Y, Guo H, Lin X, Shen C, Chen H, Dong X, Su G, and Gao H J 2022 arXiv:2209.03840 [cond-mat.supr-con]

[50] Werhahn D, Ortiz B R, Hay A K, Wilson S D, Seshadri R, and Johrendt D 2022 *Z. Naturforsch. B* **77** 757

[51] Li X, Xu X, Zhou H, Jia H, Wang E, Fu H, Sun J T, and Meng S 2023 *Nano Lett.* **23** 2839

[52] Yin Q, Tu Z, Gong C, Tian S, and Lei H 2021 *Chin. Phys. Lett.* **38** 127401

[53] Wang Q, Kong P, Shi W, Pei C, Wen C, Gao L, Zhao Y, Yin Q, Wu Y, Li G, Lei H, Li J, Chen Y, Yan S, and Qi Y 2021 *Adv. Mater.* **33** 2102813

[54] Van Hove L 1953 *Phys. Rev.* **89** 1189

[55] Huang S M, Xu S Y, Belopolski I, Lee C C, Chang G, Wang B, Alidoust N, Bian G, Neupane M, Zhang C, Jia S, Bansil A, Lin H, and Hasan M Z 2015 *Nat. Commun.* **6** 7373

[56] Qin S, Zhang Z, Wang Y, Fang C, Zhang F, and Hu J 2022 arXiv:2208.10225 [cond-mat.supr-con]

[57] Wu Z and Wang Y 2023 arXiv:2309.03285 [cond-mat.supr-con]